

1. Incorrect margins

- Margins must be 1.5 inches on left and top, and 1 inch on right and bottom.
- Common issues with margins are:
 - Margins that are much too large, especially the top.
 - A right margin that is nonexistent. The text bleeds off the page.
 - Bottom margin is too small or nonexistent. The text covers the page number.

INCORRECT - Top margin too large. Should only be 1.5 inches.

spamming *Storm botnet* [24, 50] controlled upwards of twenty million computers and gained enough computational capability (in instructions per second) to rival a supercomputer [52]. In March 2010, Microsoft obtained a restraining order to take down the servers of the Waledac botnet, which infected hundreds of thousands of computers and was capable of sending between 1 and 2 billion spam messages per day [54]

Entelecheia works by leveraging the characteristics that the P2P bots exhibit during what we call their Waiting Stage: (a) the tendency to send “keep-alive” messages to their other peers to let the botmasters know of their status and (b) the tendency to have overlapping peers due to their bootstrapping processes. Our approach produces a median F1 score of 91.8%, in a very challenging setting: (a) no signatures available, (b) no initial seeding information, (c) P2P botnets, and (d) during the Waiting stage.

The second work (detailed in Chapter 4) is focused on the the task of protecting the cyber security of an organization, which has grown increasingly more important as hackers constantly find ways to infiltrate organizations to steal valuable information. There are two common methods with which malicious entities seek to accomplish this objective, and both begin with guiding the users to websites under the control of the hackers. In the first method, the websites would either deceive the users into installing some malware into their computers or quietly execute the installation without the users knowing. In the second method, called “phishing”, the users would see a (fake) website which looks legitimate and asks for the users’ credentials to continue (think the login page of the organization’s webmail system).

We seek to address the problem by asking a key question: “*Can we detect when*

**INCORRECT - Right margin
must be at least 1 inch.**

```
aL=length(-.999:preC:.999);

Dold = inf;

Dmin = 1 +

    (q*b^2*(1+a^2-2*a*rho+sigmaQ2*(1+a^2))+2*q^2*b^2*c*(-a*sigmaQ2+((1+a^2)*rho-a*
    ...
    - 2*q*b*(1-a*rho)/(1-rho*(q*c+(1-q)*d)));

while Dmin/Dold <STOP

    %% iterate c & d

    Dold = Dmin;

    c = -.999:preC:.999; cc= repmat(c,aL,1);
    d = -.999:preC:.999; d=d'; dd= repmat(d,1,aL);
    D = 1 + (q*b^2*(1+a^2-2*a*rho+sigmaQ2*(1+a^2))...
    +
        2*q^2*b^2*cc.*(-a*sigmaQ2+((1+a^2)*rho-a*(1+rho^2))./(1-rho*(q*cc+(1-q)
    ...
        - 2*q*b*(1-a*rho)./(1-rho*(q*cc+(1-q)*dd)));
    [Dmin,i] = min(min(D)); [Dmin,j] = min(min(D'));

    c = cc(j,i); d=dd(j,i);

    %% iterate a & b
```

INCORRECT - text may not go below page number. Bottom margin must be at least 1 inch.

Algorithm 2 Hybrid MSCKF/SLAM

Propagation: Propagate the state vector

readings.

Update: Once camera measurements become available:

- Augment the state vector with the latest camera pose.
- For features to be processed in the MSCKF (feature tracks of length smaller than m), do the following
 - For each feature to be processed, calculate the residual and Jacobian in (2.19).
 - Perform the Mahalanobis gating test in (2.20).
 - Using all features that passed the gating test, form the residual vector and the Jacobian matrix in (2.22).
- For features that are included in the state vector, compute the residuals and measurement Jacobian matrices, and form the residual $\tilde{\mathbf{z}}_k$ and matrix \mathbf{H}_k in (3.2).
- Update the state vector and covariance matrix, via (3.4)-(3.7).
- Initialize features tracked in all m images of the sliding window via (3.8)-(3.10).

State Management:

- Remove SLAM features that are no longer tracked, and change the anchor pose for SLAM features anchored at the oldest poses.

- Remove the oldest IMU pose from the state. If no feature is currently tracked for more than m_o poses (with $m_o < m - 1$), remove the oldest $m - m_o$ poses.

CORRECT - margins 1.5 inches on left and top, and 1 inch on right and bottom.

CHAPTER 3 VISUAL AND CONTEXTUAL

A. Contributions

The contributions of this Chapter are: 1) A contextual disease model based on Bayesian networks to estimate the spatial location of mTBI abnormalities. It allows for a range of contextual inputs, when the exact value (time or approximate location) is not known, which could be due to patient's memory loss. This contextual model helps to overcome the low contrast appearance of mTBI by focusing on the region of the search space that may have injury. 2) A visual model that is learned using texture features to build a probabilistic support vector machine (PSVM). The method does not require registration (it is spatially invariant), which can cause distortion. 3) A novel dataset of rat MR images is developed to follow mTBI to test the validity of the proposed model. The rat controlled cortical impact (CCI) mTBI model is used with multiple observations post-injury using T2 MRI maps to demonstrate the results. This paper is an extension of [36]. It extends the approach to repeated TBI and a more in-depth analysis of the contextual inputs is given.

B. Technical Approach

1. System Overview and Technical Rationale

The proposed system is a combination of a visual and contextual model. Figure 2 shows the system diagram. A database of known mTBI MRI brain and lesion volumes with manually detected lesions and the associated contexts is used to build the model. The visual model uses 3D texture features to build a Probabilistic Support Vector

2. Incorrect page number placement

- Page numbers should be centered between the bottom line of text and the bottom of the page. About $\frac{1}{2}$ inch from the edge.
- Common Issues with page number placement:
 - The page numbers are placed too high on the page.
 - Page number touching the text.

INCORRECT - page number placed too high on the page.

them with r'_8 : **on** *ExtLgtLow* **if** $lSlp=0$ **do set** (*intLgt*, 0); resulting in model PN_{fc} . Check that the number of bad states decreases from 72,644 to 24, that the remaining problem is related to rules r_2 and r_3 . After checking **if** ($(lgt sTmr \geq 1$ **and** $lgt sTmr \leq 359)$ **and** $lMtn = 0$) **do increase** (*lgt sTmr*, 1), the model passes the check. This demonstrates the effectiveness of counterexamples to help a designer debug a set of ECA rules.

We then turn our attention to larger models, which extend our original model by introducing four additional rules and increasing variable ranges. In PN_1 and PN_2 , the external light variable *ExtLgt* ranges in $[0, 20]$ instead of $[0, 10]$; for PN_4 , it ranges in $[0, 50]$. PN_2 also extends the range of the light timer variable *lgtTmr* to $[0, 720]$; PN_3 to $[0, 3600]$. We observe that, when verifying termination or confluence, the time and memory consumption tends to increase as the model grows; also, our symbolic algorithm scales much better than the best explicit approach when verifying confluence. For the relatively small state space of PN_t , enumeration is effective, since computing TC is quite computationally expensive. However, as the state space grows, enumerating the unstable states consumes excessive resources. We also observe that the supposedly improved explicit confluence algorithm sometimes makes things worse. The reason may lie in the fact that a random selection of a state from the frontier has different statistical properties than for the original explicit approach, and also in the fact that operation caches save many intermediate results. However, both explicit algorithms run out of memory on PN_3 and PN_4 . Comparing the results for PN_3 and PN_4 , we also observe that larger state spaces might require fewer resources. With symbolic encodings, this might happen because the corresponding MDD is more regular than the one for a smaller state space.

INCORRECT - page number touching text

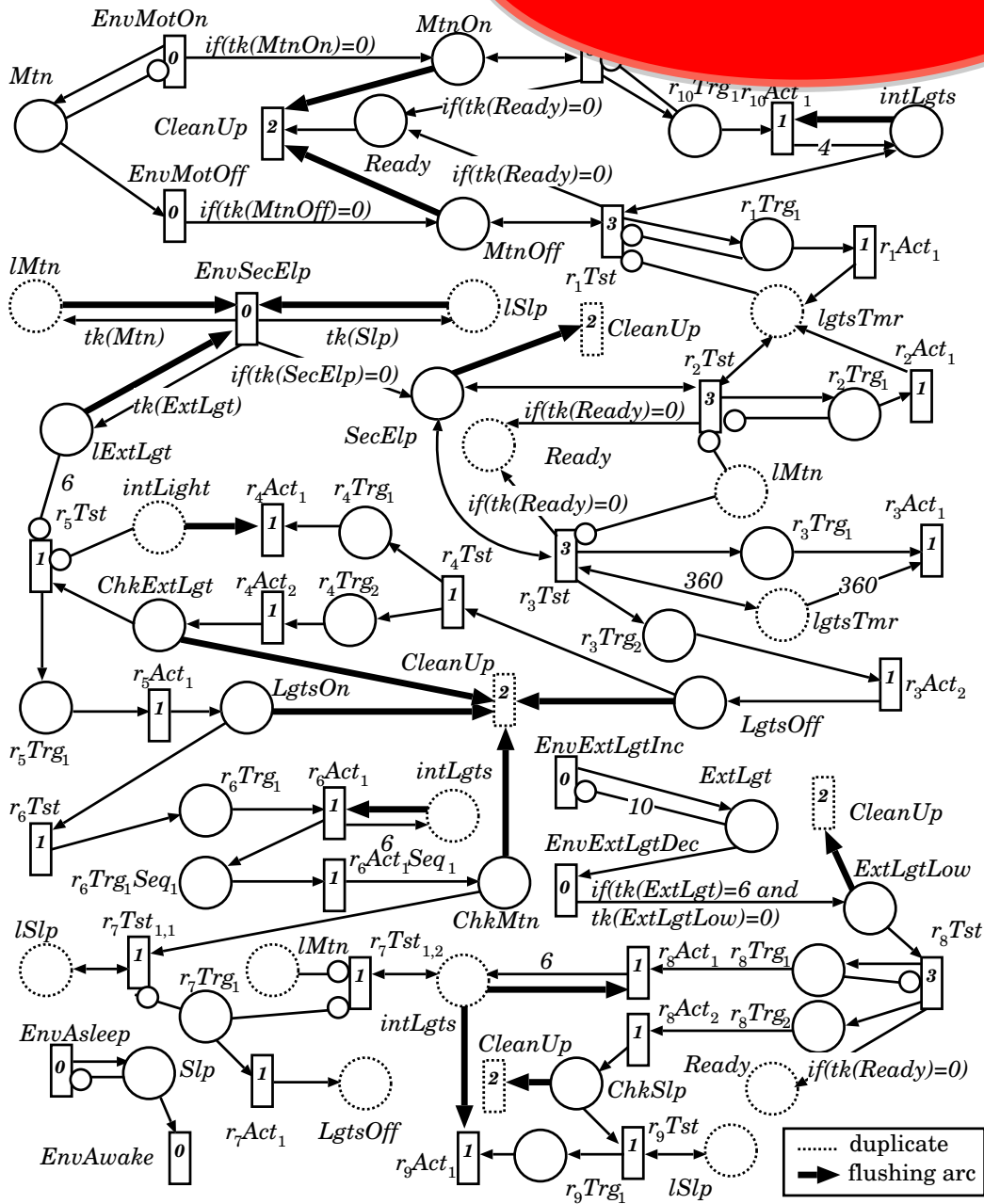


Figure 3.13: The PN for ECA rules in Figure 2.6.

3.5.1 Transforming a set of ECA rules into a PN

We now explain the procedure to transform a set of ECA rules into a PN.

First, we put each ECA rule into a regular form where both events and condition are

CORRECT - Perfect page number placement.

CHAPTER 3 VISUAL AND CONTEXTUAL

A. Contributions

The contributions of this Chapter are: 1) A contextual disease model based on Bayesian networks to estimate the spatial location of mTBI abnormalities. It allows for a range of contextual inputs, when the exact value (time or approximate location) is not known, which could be due to patient's memory loss. This contextual model helps to overcome the low contrast appearance of mTBI by focusing on the region of the search space that may have injury. 2) A visual model that is learned using texture features to build a probabilistic support vector machine (PSVM). The method does not require registration (it is spatially invariant), which can cause distortion. 3) A novel dataset of rat MR images is developed to follow mTBI to test the validity of the proposed model. The rat controlled cortical impact (CCI) mTBI model is used with multiple observations post-injury using T2 MRI maps to demonstrate the results. This paper is an extension of [36]. It extends the approach to repeated TBI and a more in-depth analysis of the contextual inputs is given.

B. Technical Approach

1. System Overview and Technical Rationale

The proposed system is a combination of a visual and contextual model. Figure 2 shows the system diagram. A database of known mTBI MRI brain and lesion volumes with manually detected lesions and the associated contexts is used to build the model. The visual model uses 3D texture features to build a Probabilistic Support Vector

3. Incorrect pagination

- The document is required to have three different sections of pagination.
 - Title/Copyright/Signature = no page numbers
 - Preliminary Pages (after signature page) = lower case roman numerals beginning with iv
 - Document = page numbers beginning with 1

**INCORRECT - no page number
on title, copyright or
signature page.**

UNIVERSITY
RIVERSIDE

Spectroscopy of Photovoltaic Materials: Charge-Transfer Complexes and
Titanium Dioxide

A Dissertation submitted in partial satisfaction
of the requirements for the degree of

Doctor of Philosophy

in

Chemistry

by

Robert J. Dillon

June 2013

Dissertation Committee:

Dr. Christopher J. Bardeen, Chairperson

Dr. Ludwig Bartels

Dr. David Bocian

INCORRECT - missing page number - lower case roman numerals used after signature page.

Acknowledgments

I thank my committee and my collaborators, without whose help, I would not have been here. I would also like to extend my gratitude to my dissertation advisor, Professor Michalis Faloutsos, who has taught me how to conduct research, how to write technical papers effectively, how to succeed outside of the academic environment, and last but not least, how to endure the challenges of the Ph.D. itself.

**INCORRECT - first page
of the document must be
page 1.**

Chapter 1

Introduction

In order to investigate the characteristics, performance metrics, and to understand the physical phenomenon behind the electronic behavior of field-effect transistors with novel channel materials, such as thin films of the transition metal dichalcogenide tantalum diselenide (TaSe_2), device fabrication and characterization were undertaken in this work. In Sec. 1.1, a brief introduction to the motivation behind radiation-hard materials for use in electronics and the device demonstrations achieved to meet the demand for radiation-hardness. In Sec. 1.2, an introduction to the proposed materials and material structure to complement silicon based devices. In Sec. 1.3, the need for low-noise devices is reviewed. In Sec. 1.4, the issues and challenges associated with device fabrication and characterization of FETs with TaSe_2 thin film channels is discussed. Finally, in Sec. 1.5, the outline of this dissertation is presented.

1.1 Radiation-hard All-metallic Logic Circuits

As motivation, scientists and engineers are continuing efforts to increase radiation hardness of electronic components. Sources of damaging ionizing radiation come from cosmic rays, x-rays, gamma rays and even alpha particle emission from radioactive contaminants of chip

4. Widow lines and Orphan headers

- There must be at least two lines of text at the top and bottom of each page.
- Pay particular attention to orphan headers = headers alone at the bottom of the page.

INCORRECT - headers with no text beneath them.

The temperature of the system is T , and $\beta = 1/(k_B T)$. The probability that a state is occupied;

$$P(\lambda_n, \beta) = \frac{e^{-\beta E_n}}{Z}$$

. The electric current is calculated using the same method as above, but including the probabilities $P(\lambda_1, \beta), P(\lambda_2, \beta)$.

$$I(t) = P(\lambda_1, \beta) \int_{p_0}^{p_f} \langle \psi_1(t) | \frac{dH}{dA} | \psi_1(t) \rangle + P(\lambda_2, \beta) \int_{p_0}^{p_f} \langle \psi_2(t) | \frac{dH}{dA} | \psi_2(t) \rangle \quad (4.71)$$

The third calculation used the density matrix formed from the wavefunctions ψ_1, ψ_2 . The time evolution of the density matrix was found from solving,

$$\begin{aligned} \dot{\rho}(t) &= -i[H, \rho] \\ \rho(0) &= \sum_n P(\lambda_n, \beta) |\psi_n(0)\rangle \langle \psi_n(0)|. \end{aligned} \quad (4.72)$$

Using the density matrix and the current operator $M = \frac{dH}{dA}$, the current element is the average of the operator (M):

$$i_p(t) = \frac{Tr[\rho M]}{Tr[\rho]}, \quad (4.73)$$

and the total current is found by summing over all momentum values,

$$I(t) = \sum_p i_p(t) \quad (4.74)$$

At extremely high temperatures, the probability functions $P(\lambda_1, \beta), P(\lambda_2, \beta)$ approach 1 and 0, respectively. The total current found from each of the three methods should be the same. The mathematica code written does show this.

At lower temperatures, the total current from the second and third methods should be identical. However, the mathematica code does not show this.

4.7 Open driven system: Linblad equation

4.8 Conclusions

INCORRECT - header with no text beneath it.

expressed in High Five cells and showed the same binding specificity as the APN receptor (Zhang et al., 2005). In contrast, APN was not involved in Cry11Aa triggering membrane insertion and pore formation (Bravo et al., 2004; Jurat-Fuentes and Adang, 2004). Therefore, I tested whether *Aedes* cadherin could mediate Cry11Aa toxicity without a secondary receptor.

Aim 1.1: Determine if *Aedes* cadherin mediates the cytotoxicity of Cry11Aa with cell line expressing *Aedes* cadherin.

Hypothesis 2: N-cadherin protein may be involved in Cry11Aa toxicity.

As mentioned above, Bti action may involve more than one mechanism or one receptor. To find more functional receptors of Bti toxins, I further investigate all cadherin proteins that are in the *Aedes* genome. Based on previous research and our microarray data, I found the N-cadherins (AAEL000597 and AAEL001196) were significantly altered in Cry11Aa-treated larvae midgut. Therefore, I investigated whether N-cadherin is involved in Cry11Aa toxicity. I first tested whether N-cadherins bind Cry11Aa and N-cadherin-silenced larvae obtain tolerance to Cry11Aa toxicity. Moreover, I investigated which regions are interacted between Cry11Aa and N-cadherin.

Aim 2.1: Test whether Cry11Aa binds to N-cadherin since Cry11Aa binds to normal cadherin proteins.

5. No spaces between references and list entries

- References should be single spaced with a blank line between each.
- The List of Figures and List of Tables must have a blank line between each entry.

**INCORRECT - there must be
a blank line (double space)
between each reference**

13. Zhang, P., et al. *Navigation with IMU/GPS using unscented Kalman filter*. in *Mechatronics and Automation, 2005 IEEE International Conference*. 2005. IEEE.
14. Yi, Y. and D. Grejner-Brzezinska. *Tightly-coupled GPS/INS integration using unscented Kalman filter and particle filter*. in *Proceedings of the 19th International Technical Meeting of the Satellite Division of The Institute of Navigation (ION GNSS 2006)*. 2001.
15. Giremus, A., et al., *A Rao-Blackwellized particle filter for INS/GPS integration*. 2004.
16. Gross, J., et al. *A comparison of extended kalman filter, sigma-point kalman filter, and particle filter in GPS/INS sensor fusion*. in *AIAA Guidance, Navigation, and Control Conference*. 2010.
17. Schmidt, G.T. and R.E. Phillips, *INS/GPS Integration Architecture Performance Comparisons*. *Advances in Navigation Sensors and Integration Technology*.
18. Farrell, J. and M. Barth, *The global positioning system and inertial navigation*. Vol. 61. 1999: McGraw-Hill New York.
19. Dai, L., et al. *Pseudolite applications in positioning and navigation: Modelling and geometric analysis*. in *Int. Symp. on Kinematic Systems in Geodesy, Geomatics & Navigation (KIS2001)*. 2001.
20. de Lara, E. and S. Saroiu. *CILoS: a CDMA indoor localization system*. in *Proceedings of the 10th international conference on Ubiquitous computing*. 2008. ACM.
21. Otsason, V., et al., *Accurate GSM indoor localization*, in *UbiComp 2005: Ubiquitous Computing*. 2005, Springer. p. 141-158.
22. Wang, X., Y. Wu, and J.-Y. Chouinard, *A new position location system using DTV transmitter identification watermark signals*. *EURASIP Journal on Applied Signal Processing*, 2006. **2006**: p. 155-155.
23. Rabinowitz, M. and J.J. Spilker Jr, *A new positioning system using television synchronization signals*. *Broadcasting, IEEE Transactions on*, 2005. **51**(1): p. 51-61.
24. Youssef, A., et al. *Computing location from ambient FM radio signals [commercial radio station signals]*. in *Wireless Communications and Networking Conference, 2005 IEEE*. 2005. IEEE.
25. Popleteev, A., *Indoor positioning using FM radio signals*. 2011, University of Trento.
26. Hall, T.D., C.C. Charles III, and P.N. Misra. *Radiolocation using AM broadcast signals: Positioning performance*. in *Proceedings of the 15th International Technical Meeting of the Satellite Division of The Institute of Navigation (ION GPS 2002)*. 2001.
27. Evennou, F. and F. Marx, *Advanced integration of WiFi and inertial navigation systems for indoor mobile positioning*. *Eurasip journal on applied signal processing*, 2006. **2006**: p. 164-164.
28. sYe, X., *WiFiPoz--an accurate indoor positioning system*. 2012.

**CORRECT - blank line
between each reference**

- [13] Naranjo, J.E.; Bouraoui, L.; Garcia, R.; Parent, J., "Control Architecture for Cybercars and Dual-Mode Cars," *Intelligent Transportation Systems, IEEE Transactions on*, vol.10, no.1, pp.146,154, March 2009
- [14] Vi Tran Ngoc Nha; Djahel, S.; Murphy, J., "A comparative study of vehicles' routing algorithms for route planning in smart cities," *Vehicular Traffic Management for Smart Cities (VTM), 2012 First International Workshop on*, vol., no., pp.1,6, 20-20 Nov. 2012
- [15] Zhan, F.B.; Noon, C.E. Shortest Path Algorithms: An Evaluation Using Real Road Networks. *Transportation Science* 1998, 32, 65–73.
- [16]. Cao, L.; Shi, Z.; Bao, P. Self-adaptive Length Genetic Algorithm for Urban Rerouting Problem. In *Advances in Natural Computation*; Jiao, L.; Wang, L.; Gao, X.b.; Liu, J.; Wu, F., Eds.; Springer Berlin Heidelberg, 2006; Vol. 4221, Lecture Notes in Computer Science, pp. 726–729.
- [17]. Dorigo, M.; Stützle, T. *Ant Colony Optimization*; MIT Press, Cambridge MA, 2004
- [18] Glover, F.; Laguna, M. Tabu Search. *Journal of computational biology a journal of computational molecular cell biology* 1997, 16, 1689–703.
- [19] Frazzoli, E.; Bullo, F., "Decentralized algorithms for vehicle routing in a stochastic time-varying environment," *Decision and Control, 2004. CDC. 43rd IEEE Conference on*, vol.4, no., pp.3357,3363 Vol.4, 14-17 Dec. 2004
- [20] Francesco Bullo, Jorge Cortés, Sonia Martínez, *Distributed Control of Robotic Networks A Mathematical Approach to Motion Coordination Algorithms - Chapter 2: Geometric models and optimization*, Princeton University Press, 2009
- [21] Lujak, M.; Giordani, S.; Ossowski, S., "Fair route guidance: Bridging system and user optimization," *Intelligent Transportation Systems (ITSC), 2014 IEEE 17th International Conference on*, vol., no., pp.1415,1422, 8-11 Oct. 2014.
- [22] Alesiani, F.; Maslekar, N., "Optimization of Charging Stops for Fleet of Electric Vehicles: A Genetic Approach," *Intelligent Transportation Systems Magazine, IEEE*, vol.6, no.3, pp.10,21, Fall 2014.
- [23] Garg, A.; Pandey, K.; Singh, B., "Hierarchical map-based location service for VANETs in urban environments," *Contemporary Computing (IC3), 2014 Seventh International Conference on*, vol., no., pp.199,205, 7-9 Aug. 2014.

6. Co-Chairpersons on dissertation committee

- Example of “Chairperson”
- Example of “Co-Chairperson” configuration

CORRECT - one chairperson is listed this way.

UNIVERSITY OF CALIFORNIA
RIVERSIDE

Computational Methods for Mild Traumatic Brain Injury

A Dissertation submitted in partial satisfaction
of the requirements for the degree of

Doctor of Philosophy

in

Electrical Engineering

by

Anthony Christopher Bianchi

December 2014

Dissertation Committee:

Dr. Bir Bhanu, Chairperson

Dr. Andre Obenaus

Dr. Hyle Park

CORRECT - if you have co-chairperons, they must be listed this way.

UNIVERSITY OF CALIFORNIA
RIVERSIDE

Pathophysiology of Juvenile Traumatic Brain Injury:
Role of Edema and a Potential Treatment

A Dissertation submitted in partial satisfaction
of the requirements for the degree of

Doctor of Philosophy

in

Neuroscience

by

Arash Matthew Adami

August 2013

Dissertation Committee:

Dr. Andre Obenaus, Co-Chairperson

Dr. Margarita Curras-Collazo, Co-Chairperson

Dr. Michael Adams